

Single crystal growth and characterizations of $\text{Cu}_{0.03}\text{TaS}_2$ superconductors

X.D. Zhu^a, Y.P. Sun^{a,b,*}, X.B. Zhu^a, X. Luo^a, B.S. Wang^a, G. Li^a, Z.R. Yang^a, W.H. Song^a, J. M.

Dai^a

^aKey Laboratory of Materials Physics, Institute of Solid State Physics, Chinese Academy of Sciences, Hefei 230031, People's Republic of China

^bHigh Magnetic Field Laboratory, Chinese Academy of Sciences, Hefei 230031, People's Republic of China

Abstract

Single crystal of $\text{Cu}_{0.03}\text{TaS}_2$ with low copper intercalated content was successfully grown via chemical vapor transport method. The structural characterization results show that the copper intercalated $2H\text{-Cu}_{0.03}\text{TaS}_2$ single crystal has the same structure of the CdI_2 -type structure as the parent $2H\text{-TaS}_2$ crystal. Electrical resistivity and magnetization measurements reveal that $2H\text{-Cu}_{0.03}\text{TaS}_2$ becomes a superconductor below 4.2 K. Besides, electrical resistivity and Hall effects results show that a charge density wave transition occurs at $T_{\text{CDW}} = 50$ K.

PACS: 81.10.-h; 81.10.Bk; 74.70.-b

Keywords: A1. Charge density wave; A2. Single crystal growth; A2. Chemical vapor transport; B2. Superconducting materials.

* Corresponding author. Tel.: +86 551 559 2757; Fax: +86 551 559 1434.

E-mail address: ypsun@issp.ac.cn

1. Introduction

Diverse physical properties such as Charge-Density-Wave (CDW) and superconductivity in layered transition metal dichalcogenides (TMDC) have been broadly studied [1, 2]. TMDC have a general formula TX_2 , where T is usually a transition metal atom from group of IVB, VB, VIB of the periodic table of elements and X is one of sulfur, selenium, or tellurium. The layered TMDC can be regarded as stacking two-dimensional X-T-X sandwiches. The bonding within each sandwich is covalent, while the bonding between them is weak van der Waals type. The crystal structures of the layered TMDC are usually described as $1T$, $2H$, $3R$, $4H_a$, $4H_b$, $6R$ phases [1, 2]. The integer denotes the number of X-T-X layers per unit cell perpendicular to the layers, while T , H , and R denote trigonal, hexagonal, rhombohedral symmetries, respectively.

Introducing foreign atoms or molecules between the weak coupling sandwiches or layers is the process of intercalation. Intercalation not only increases the layer separation, but also provides a powerful way to tune the electronic structures of the host materials. Intercalated TMDC, graphite, and layered structural transition metal nitrides have received considerable attention due to their special structures and transport properties especially for superconductivities [2-4]. New interests have been aroused since the recent discoveries of superconductivities in YbC_6 , CaC_6 and Cu_xTiSe_2 [5-7].

$2H-TaS_2$ is one of the layered TMDC [8]. Metallic $2H-TaS_2$ undergoes a CDW transition at 78K, and becomes a superconductor below 0.8 K [8]. Many inorganic atoms and organic molecules have been intercalated into TaS_2 [3, 9-14]. Intriguingly, superconductivity has been found in $Py_{1/2}TaS_2$ [9], $A_{0.33}TaS_2$ ($A = Li, Na, K, Rb, Cs$) [14], and $2H-Fe_xTaS_2$ ($x = 0.05$) et al. [15]. Recently, the competition driven by intercalation between superconductivity and CDW in Na_xTaS_2 has been discovered [16]. Copper intercalations in TaS_2 have been achieved by chemical vapor transport (CVT) method to produce $Cu_{1/2}TaS_2$ [17], by direct reaction from copper and TaS_2 to produce single phase Cu_xTaS_2 ($0.33 < x < 0.75$) [18], and by electro-chemical method [19]. However, superconductivity has not been observed in any high copper intercalation Cu_xTaS_2 [17-19]. Further, there is also no any report about lower copper intercalation in Cu_xTaS_2 . Thus, it is interesting to explore whether low copper intercalation in Cu_xTaS_2 can induce superconductivity or not. The low copper intercalation experiments were carried out in order to search for possible superconductivity

in Cu_xTaS_2 ($x < 0.33$). In this paper, we report the single crystal growth of $\text{Cu}_{0.03}\text{TaS}_2$ with low copper intercalated content via CVT method. Electrical resistivity and magnetization measurements reveal that $2H\text{-Cu}_{0.03}\text{TaS}_2$ becomes a superconductor below 4.2 K. Besides, resistivity and Hall effects results show that a charge density wave transition occurs at $T_{\text{CDW}} = 50$ K.

2. Experimental procedure

Single crystal $\text{Cu}_{0.03}\text{TaS}_2$ was grown via CVT method. Firstly, polycrystalline TaS_2 powder was synthesized by solid state reaction. Stoichiometric amounts of Ta and S powders were mixed and sealed in an evacuated quartz tube. The tube was heated at 900°C for 4 days. Secondly, Cu, TaS_2 powders in mol ratio of 0.5:1, and 100 mg iodine were mixed and sealed in an evacuated quartz tube with a 12 mm diameter and a 19 cm length. The tube was inserted in a two-zone horizontal tube furnace with a source-zone temperature of 1000°C and a growth-zone temperature of 900°C for 10 days. Both zones were decreased to 440°C in several days, and then cooled to room temperature. Dark blue, mirror-like plates in a typical size of $3 \times 3 \times 0.2 \text{ mm}^3$ were obtained, and the photograph is shown in Fig. 1. F. R. Gamble et al. has reported that $2H\text{-TaS}_2$ single crystals grown via CVT method were black and somewhat wrinkle [9].

The grown $\text{Cu}_{0.03}\text{TaS}_2$ plates were cleaned by ultrasonic in supersaturated aqueous solutions of KI, de-ionized water, and alcohol, respectively. The composition of $\text{Cu}_{0.03}\text{TaS}_2$ single crystal was characterized by energy dispersive x-ray spectroscopy (EDS) and inductively coupled plasma atomic emission spectrometry (ICP-AES, Atomscan Advantage). The crystal structure and phase purity were examined by powder and single-crystal X-ray diffraction pattern (XRD) using a Philips X' pert PRO x-ray diffractometer with Cu $K\alpha$ radiation at room temperature. The electrical resistivity was performed by the standard four-probe method using a Quantum Design Physical Property Measurement System (PPMS) ($1.8 \text{ K} \leq T \leq 400 \text{ K}$, $0 \text{ T} \leq H \leq 9 \text{ T}$). The Hall effects experiments were also performed using PPMS. Magnetization measurements as a function of temperature were performed in a Quantum Design Superconducting Quantum Interference Device (SQUID) system ($1.8 \text{ K} \leq T \leq 400 \text{ K}$, $0 \text{ T} \leq H \leq 5 \text{ T}$).

3. Results and discussions

3.1. Chemical analysis

The EDS pattern for the grown single crystal is shown in Fig. 2. The estimated mol ratio of Ta : S is about 1 : 2. Though the copper peak is evident in the EDS spectrum, the accurate copper content can not be obtained because the copper content is too small. Thus, the copper content is determined by ICP-AES. The determined mol ratio of the Cu : Ta is 0.03 : 1.

3.2. Structural analysis

The XRD patterns for $\text{Cu}_{0.03}\text{TaS}_2$ and $2H\text{-TaS}_2$ single crystals are shown in Fig. 3a. It can be observed that the orientations of the crystal surfaces are both (001) planes. The magnification plots of (006) peaks are shown in the inset of Fig. 3a. Obviously, the peak positions of $\text{Cu}_{0.03}\text{TaS}_2$ shift to lower 2θ value. According to the Bragg equation $n\lambda = 2d\sin\theta$, the copper intercalation leads to expansion of the lattice constant c .

Several single crystals were crushed into powders, which were used in the powder XRD experiment. The powder XRD patterns of crushed $\text{Cu}_{0.03}\text{TaS}_2$ and $2H\text{-TaS}_2$ crystals are shown in Fig. 3b. All the peaks can be well indexed to the $2H$ structure [20]. The present $\text{Cu}_{0.03}\text{TaS}_2$ is single phase with no detectable secondary phases. The lattice constants were obtained from powder XRD patterns. The lattice constant of $\text{Cu}_{0.03}\text{TaS}_2$ is almost equal to that of $2H\text{-TaS}_2$ ($a = 3.31\text{\AA}$), while the lattice constant c of $\text{Cu}_{0.03}\text{TaS}_2$ is $12.13(7)\text{\AA}$, which is slightly larger than that of $2H\text{-TaS}_2$ ($c = 12.08(0)\text{\AA}$).

3.3. Co-existence of superconductivity and charge density wave

The temperature dependence of electrical resistivity in ab plane ($\rho_{ab}\text{-}T$) for $2H\text{-Cu}_{0.03}\text{TaS}_2$ is plotted in Fig. 4. Obviously, there is a kink around $T = 50\text{ K}$, which can be attributed to CDW transition. The inset shows the enlarged view of the $\rho_{ab}\text{-}T$ curve near the superconducting region. The resistivity sharply drops to zero around $T = 4.2\text{ K}$, which indicates the superconductivity. The onset superconducting transition temperature is 4.2 K , and the transition width (10%-90%) is 0.2 K .

The temperature dependence of dc magnetic susceptibility for $\text{Cu}_{0.03}\text{TaS}_2$ is plotted in Fig. 5. The magnetic field of 2 Oe was applied parallel to the ab plane of a $\text{Cu}_{0.03}\text{TaS}_2$ plate. A sharp drop of magnetization at 4.2 K was observed for both zero-field-cooling (ZFC) and field-cooling (FC) measurements, which further confirms the existence of superconductivity. The ZFC curve shows an almost perfect shielding effect, while the magnetic flux exclusion fraction estimated from the FC curve is as low as $\sim 4\%$ at 2 K, using $-4\pi\chi_v$ to estimate the volume fraction. Similar phenomena have been reported in other intercalated compounds such as $\text{Py}_{1/2}\text{TaS}_2$ [21], YbC_6 and CaC_6 [5, 6], LiPd_3B_2 [22]. Prober *et al.* suggested that the small FC magnetization was due to the complicated flux trapping effect in these intercalated compounds [23]. Thus, it is suggested that the bulk superconductivity is found in $\text{Cu}_{0.03}\text{TaS}_2$.

The temperature dependence of the Hall (R_H) coefficient for $\text{Cu}_{0.03}\text{TaS}_2$ is shown in the Fig. 6. The R_H versus T is determined from the Hall resistivity (ρ_{xy}) results using $R_H = \rho_{xy}/H$. The inset in Fig. 6 shows the magnetic field dependence of the ρ_{xy} measured at different temperatures. The R_H increases from $\sim 2.8 \times 10^{-4} \text{cm}^3/\text{C}$ above 60 K to $\sim 5.5 \times 10^{-4} \text{cm}^3/\text{C}$ below 30K. In contrast, the sign of the R_H of matrix $2H\text{-TaS}_2$ even change from positive to negative near the CDW transition, which was reported by A. H. Thompson et al [21]. The change of the R_H of $\text{Cu}_{0.03}\text{TaS}_2$ in the region of $30 \text{ K} < T < 60 \text{ K}$ confirms the CDW transition revealed by the resistivity results. Apparently, copper intercalation suppresses the T_{CDW} from $T_{\text{CDW}} \sim 78 \text{ K}$ ($2H\text{-TaS}_2$) to $T_{\text{CDW}} \sim 50 \text{ K}$. According to the formula $n_H = -\frac{1}{eR_H}$, the reduction of carrier density is consistent with the partial gapping of the Fermi surface due to the occurrence of CDW transition.

4. Conclusion

In summary, $\text{Cu}_{0.03}\text{TaS}_2$ single crystals with low copper intercalated content was successfully grown via CVT. Structure analysis shows that the low copper intercalated $\text{Cu}_{0.03}\text{TaS}_2$ and the parent compound $2H\text{-TaS}_2$ share the same structure. Electrical resistivity and magnetization measurements reveal that $2H\text{-Cu}_{0.03}\text{TaS}_2$ becomes a superconductor below 4.2 K. Besides, electrical resistivity and

Hall effects results show that a charge density wave transition occurs at $T_{\text{CDW}} = 50$ K.

Acknowledgements

This work was supported by the National Key Basic Research under contract No. 2006CB601005, 2007CB925002, and the National Nature Science Foundation of China under contract No.10774146, 10774147 and Director's Fund of Hefei Institutes of Physical Science, Chinese Academy of Sciences.

References

- [1] J. A. Wilson and A. D. Yoffe, *Adv. Phys.* 18 (1969) 193.
- [2] R. H. Friend and A. D. Yoffe, *Adv. Phys.* 36 (1987) 1.
- [3] M. S. Dresselhaus and G. Dresselhaus, *Adv. Phys.* 56 (2002) 1.
- [4] S. Yamanaka, *Annu. Rev. Mater. Sci.* 30 (2000) 53.
- [5] T. E. Weller, T. E. Weller, M. Ellerby, S. S. Saxena, R. P. Smith, and N. T. Skipper, *Nature Physics* 1 (2005) 30.
- [6] N.E mery, C. Hérold, M. d'Astuto, V. Garcia, Ch. Bellin, J. F. Marêché, P. Lagrange, and G. Loupiau, *Phys. Rev. Lett.* 95 (2005) 087003.
- [7] E. Morosan, H. W. Zandbergen, B. S. Dennis, J. W. G. Bos, Y. Onose, T. Klimczuk, A. P. Ramirez, N. P. Ong and R. J. Cava, *Nature Physics* 2 (2006) 544.
- [8] J. M. E. Harper, T. H. Geballe and F. J. Di Salvo, *Phys. Rev. B* 15 (1977), 2943.
- [9] F. R. Gamble, F. J. Di Salvo, R. A. Klemm and T. H. Geballe, *Science* 168 (1970) 568.
- [10] D. W. Murphy, F. J. Di Salvo, G. W. Hull, and J. V. Waszczak, *Inorganic Chemistry* 15 (1976) 17.
- [11] R. M. Fleming and R. V. Coleman, *Phys. Rev. Lett.* 34 (1975) 1502.
- [12] A. Schlicht, A. Lerf and W. Biberacher, *Synthetic Metals* 102 (1999) 1483.
- [13] S. F. Meyer, R. E. Howard, G. R. Stewart, J. V. Acrivos, and T. H. Geballe, *J. Chem. Phys.* 62 (1975) 4411.

- [14] A. Lurf, F. Sernetz, W. Biberacher, R. Schöllhorn, *Mat. Res. Bull.* 14 (1979) 797.
- [15] R. M. Fleming and R. V. Coleman, *Phys. Rev. Lett.* 34 (1975) 1502.
- [16] L. Fang, Y. Wang, P. Y. Zou, L. Tang, Z. Xu, H. Chen, C. Dong, L. Shan, and H. H. Wen, *Phys. Rev. B* 72 (2005) 014534.
- [17] R. de Ridder, G. van Tendeloo, J. van Landuyt, D. van Dyck, and S. Amelinckx, *Phys. Stat. Sol. (a)* 37 (1976) 691.
- [18] T. Uchida, S. Sato, M. Wakihara and M. Taniguchi, *Nippon Kagaku Kaishi* 10 (1991) 1306.
- [19] C. Ramos, A. Lurf and T. Butz, *Hyperfine Interactions* 61 (1990) 1209.
- [20] A. Meetsma, A. Meetsma, G. A. Wiegers, R. J. Haange and J. L. de Boer, *Acta. Cryst. C* 46 (1990) 1598.
- [21] A. H. Thompson, F. R. Gamble and R. F. Koehler, Jr. *Phys. Rev. B* 5 (1972) 2811.
- [22] K. Togano, P. Badica, Y. Nakamori, S. Orimo, H. Takeya, and K. Hirata, *Phys. Rev. Lett.* 93 (2004) 247004.
- [23] D. E. Prober and M. R. Beasley and R. E. Schwall, *Phys. Rev. B* 15 (1977) 5245.

Figure Captions:

Fig. 1. Photograph of $\text{Cu}_{0.03}\text{TaS}_2$ single crystal.

Fig. 2. The EDS pattern for $\text{Cu}_{0.03}\text{TaS}_2$.

Fig. 3. The single crystal XRD patterns for $\text{Cu}_{0.03}\text{TaS}_2$ and $2H\text{-TaS}_2$; Inset: the magnification plot of single crystal XRD patterns; (b) The powder XRD patterns for $\text{Cu}_{0.03}\text{TaS}_2$ and $2H\text{-TaS}_2$.

Fig. 4. Temperature dependence of the in-plane resistivity (ρ_{ab}) for $\text{Cu}_{0.03}\text{TaS}_2$. The inset shows the $\rho_{ab}\text{-}T$ curve near the superconducting region. The arrows show the charge density wave transition temperature (T_{CDW}) and the onset transition temperature (T_{Conset}).

Fig. 5. The temperature dependence of ZFC and FC susceptibility χ_g measured in an applied field of 2 Oe parallel to ab plane for $\text{Cu}_{0.03}\text{TaS}_2$: FC (filled circles); ZFC (open circles).

Fig. 6. Temperature dependence of the Hall coefficients (R_H) for $\text{Cu}_{0.03}\text{TaS}_2$. The inset shows the measured Hall resistivity (ρ_{xy}) versus H measured at different temperatures.

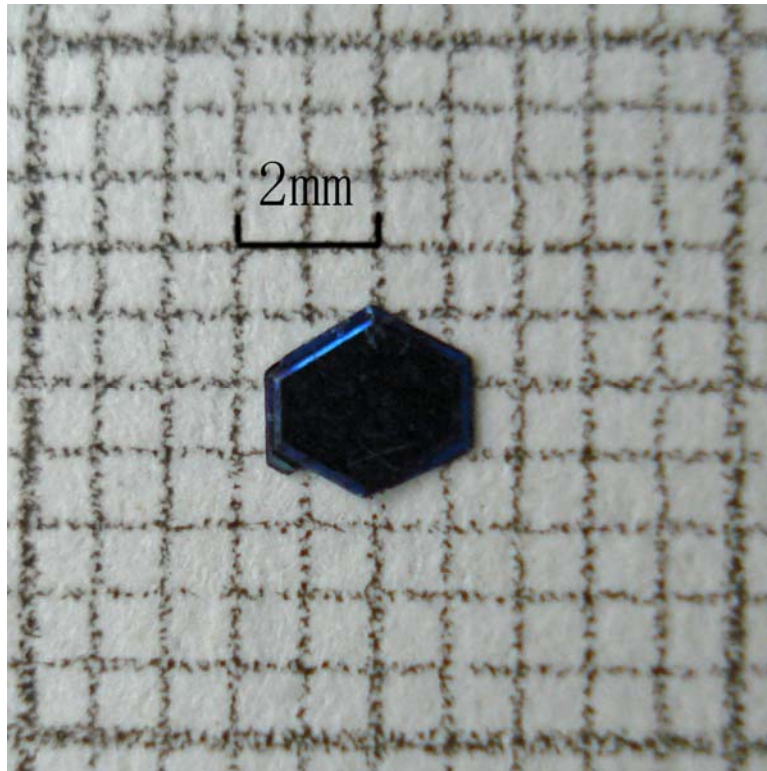


Fig. 1 X D.Zhu et al

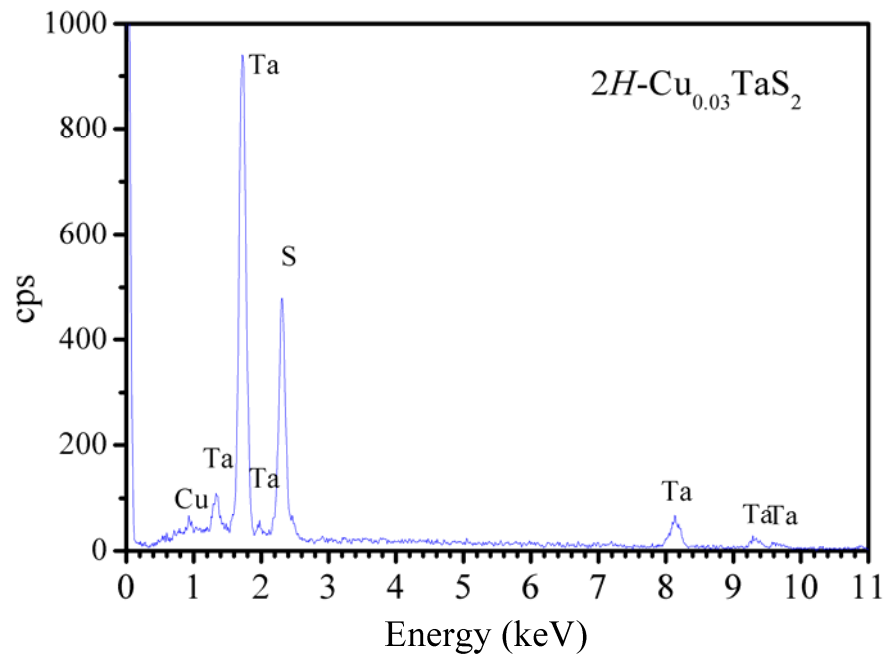


Fig. 2 X D.Zhu et al

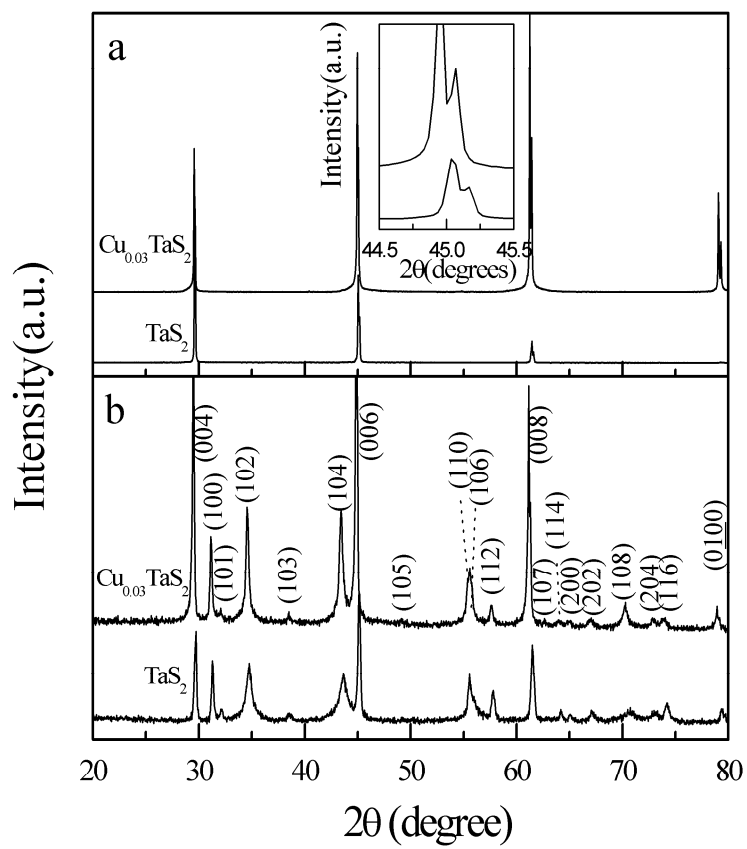


Fig. 3 X D.Zhu et al

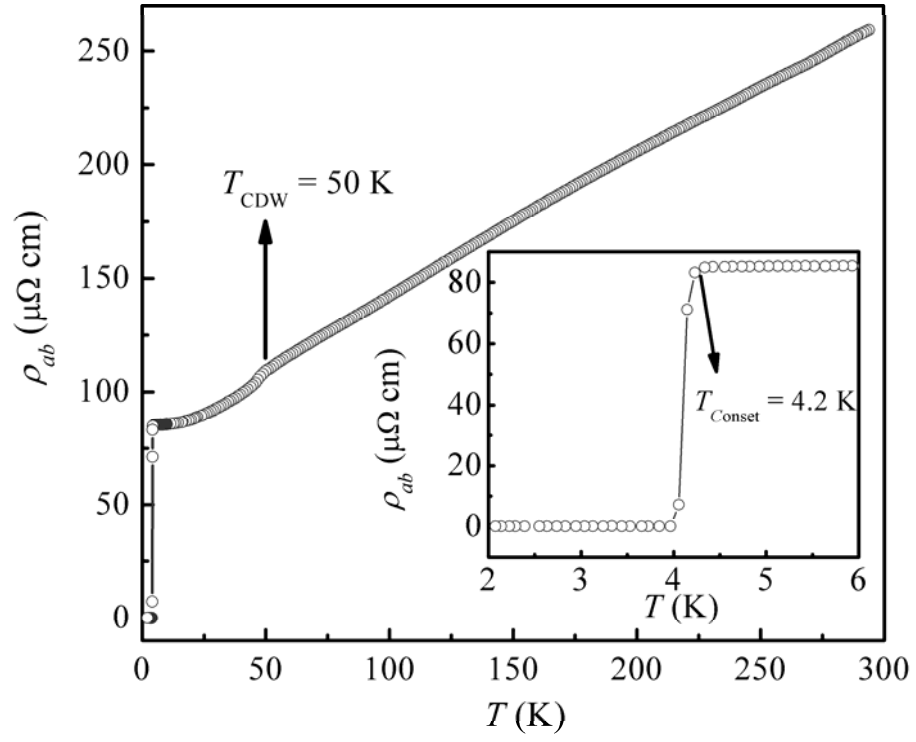


Fig. 4 X D.Zhu et al

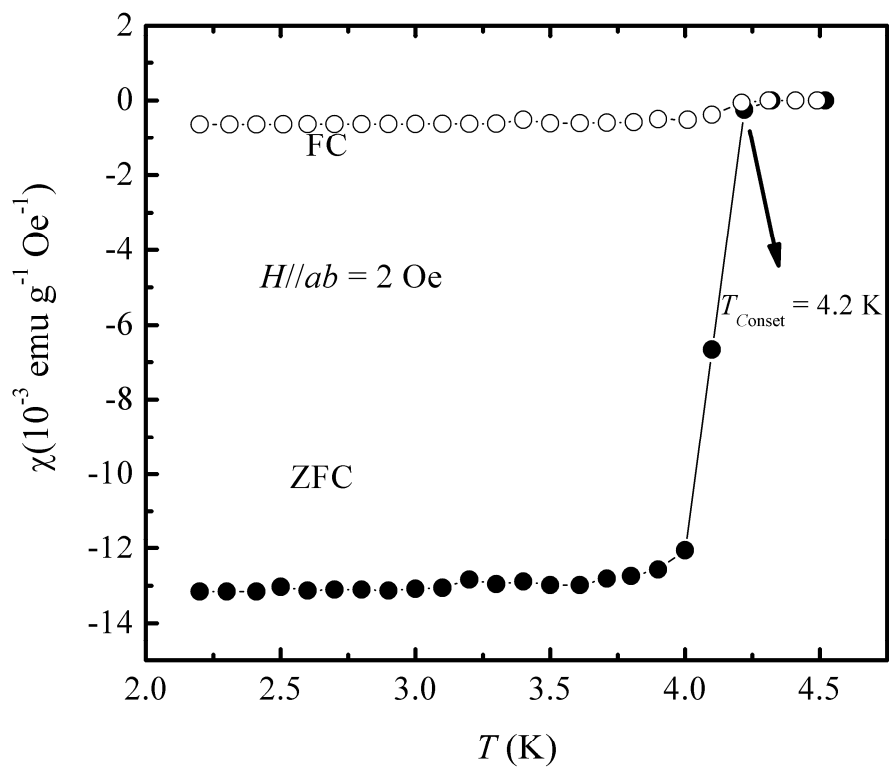


Fig. 5 X D.Zhu et al

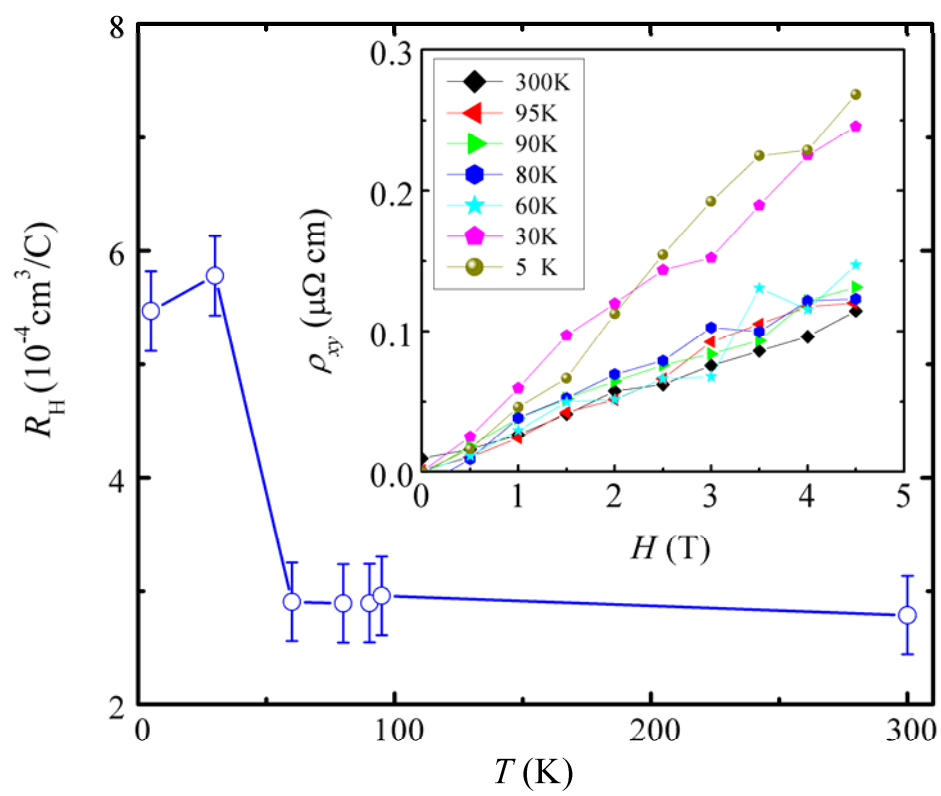


Fig. 6 X D.Zhu et al